Article:
Al-Sallami, W, Al-Damook, A and Thompson, HM (2016) A Numerical Investigation of Thermal Airflows over Strip Fin Heat Sinks. International Communications in Heat and Mass Transfer, 75. pp. 183-191. ISSN 0735-1933

https://doi.org/10.1016/j.icheatmasstransfer.2016.03.014

A Numerical Investigation of Thermal Airflows over Strip Fin Heat Sinks

Waleed Al-Sallami[1,*], Amer Al-Damook[1, 2], H.M. Thompson[1]

[1]School of Mechanical Engineering, University of Leeds, UK

[2]Mechanical Engineering Department, Faculty of Engineering, University of Anbar, Iraq,

*Corresponding Author: waleedalsallami@gmail.com

Abstract

The benefits of using strip fin heat sinks (SFHSs) where the cross-sectional aspect ratio of the fins lie between those for plate fins (high aspect ratio) and pins fins (aspect ratio≈ 1) are explored computationally, using a conjugate heat transfer model. Results show that strip fins provide another effective means of enhancing heat transfer, especially when staggered arrangements of strip fins are used. A detailed parameter investigation demonstrates that perforating the strip fins provide additional improvements in terms of enhanced heat transfer, together with reduced pressure loss and heat sink mass. Results are also given which show that, for practical applications in micro-electronics cooling, perforated SFHSs offer important benefits as a means of achieving smaller processor temperatures for reduced mechanical power consumption.

Keywords: perforations, k-ω SST model, conjugate heat transfer and heat dissipation rate.

NOMENCLATURE			
A_c	cross-sectional area of the flow passage of the heat sink, m^2	Re	Reynolds number
D	pin diameter of the pin fin heat sink, mm	T	temperature, ^oC
d	perforation diameter of the pin fin, mm	ΔT	temperature difference, ^oC
D_h	hydraulic diameter, m	U	air velocity, m/s
H	pin fin height, mm	θ_s	thermal resistance in terms of surface area, K m^2/W
θ	Thermal resistance, K/W	T_{base}	Base temperature, ^0C
h_p	Projected heat transfer coefficient	h_T	Total heat transfer coefficient
h	heat transfer coefficient, W/m^2.K	**Greek**	
k	turbulence kinetic energy	α	fluid thermal diffusivity (m^2/s)
n	number of perforations	α,β,β*	turbulence model constant
N	number of pins	ϕ	porosity V_{void}=V
L	heat sink length, mm	μ	fluid viscosity (Pa·s)
Nu	Nusselt number	μ_t	turbulent eddy viscosity, Pa.s
P	fan power, W	ρ	fluid density (kg/m^3)
Δp	pressure drop, Pa	ν	kinematic viscosity, m^2/s
Pr	Prandtl number	$_{vt}$	turbulent kinematic viscosity, m^2/s
Pr_t	turbulent Prandtl number	σ_ε	k-ε turbulence model constant
Q	power applied on the base, W	σ	turbulence model constant for the k-equation
S_z	pin pitch in streamwise direction, mm	ω	k-ω turbulence model constant

1. INTRODUCTION

The inexorable rise in heat flux densities from micro-electronic components and devices is presenting the industry with formidable challenges in maintaining processor temperatures below critical values, in order to circumvent a range of important failure modes, [1]. These challenges have stimulated a number of cooling innovations, including the use of highly conductive inserts to provide more efficient pathways to heat removal, [2], and a number of promising liquid cooling methods. The latter include on-chip cooling, direct liquid jet impingement and dielectric liquid immersion which removes heat by convection currents, [3].

This paper focusses on what remains currently the most popular approach for cooling microelectronics, namely convective heat transfer to air as it flows over a network of extended surface fins on a heat sink. It has recently been estimated that heat sinks account for more than 80% of the thermal management solutions for electronics, which will be worth over $10 billion in 2016 [4]. Heat sinks provide a low cost and reliable means of achieving a large total heat transfer surface area without excessive primary surface area, and the surface fins act as turbulence promoters which enhance heat transfer rates by breaking up the thermal boundary layer. The main goals of heat sink design are to provide sufficient heat transfer rates, to ensure processor temperatures remain below critical values, for minimal pressure loss and heat sink mass, see e.g. [5].

Heat sinks based on rectangular plate fins (PFHSs) are the most common. Several experimental and numerical studies of PFHSs have appeared in the literature, see e.g. [6, 7], and these have demonstrated that the heat transfer rate can be improved by modifying the arrangement of the fins by, for example, employing staggered arrangements of plate fins, see e.g. [8, 9], or periodically interrupted diverging and converging fins, [10]. Generally, it is found that staggered arrangements of plate fins can improve heat transfer but at the cost of significantly larger pressure drops across the PFHSs.

A number of recent studies have shown that perforating the fins in PFHSs can lead to localised air jets which result in substantial improvements in heat transfer rate with reduced pressure losses. Shaeri and Yaghoubi [11], Dhanawade and Dhanawade [12] studied thermal air flows through arrays of plate fins, with one or more rectangular or perforations respectively parallel to the dominant flow direction. They found that perforations reduce the pressure loss by reducing the size of the wakes behind the fins and the length of the recirculation zone around the lateral surface of the fins, whereas air jets through the

perforations generally enhance the heat transfer rate. Ismail et al [13] also found that the shape of the perforations can be influential and that the pressure drop with circular perforations is substantially smaller than with square ones.

The plate fins on heat sinks are often replaced by pins with a much smaller cross-sectional aspect ratio, typically with the ratio of fin length to width AR≈1, see Fig. 1. These are often referred to as Pinned Heat Sinks (PHSs) and several studies have shown that PHSs can be much more effective at disrupting the boundary layer and improving rates of heat transfer, see e.g. [14], [15], but at the cost of much larger pressure drops. The effect of pin arrangement in terms of pin density and orientation to the dominant flow direction (either in-line or staggered) has also been shown to be very influential in PHSs. Generally, increasing pin density and employing staggered arrangements of pins both lead to increased rates of heat transfer and larger pressure losses, [8, 16-19].

In comparison with PFHSs, relatively few studies have considered the effect of perforations on heat transfer and pressure drops in PHSs. Sahin and Demir [20, 21], for example, studied the effect of cross-sectional shape (circular or square) for in-line pin arrays while Dhumne and Farkade [9] considered the effect of staggered pin arrangements for singly-perforated pins of circular cross-section. Dai [22] studied the benefits of micro-jets to improve heat transfer rate and reduce pressure drop by inducing flow separation in PHSs. Collectively, these studies have shown that perforations can also lead to substantial improvements in heat transfer for reduced pressure losses for PHSs. Al-Damook et al [15] have very recently used complementary experimental and numerical methods to explore the benefits of using multiple pin perforations within PHSs. They showed that the heat transfer rate increases monotonically with the number of pin perforations, while the pressure drop and fan power, required to overcome the pressure drop, both reduce monotonically; the location of the perforations were found to be much less influential. Their conjugate heat transfer analysis showed, further, that improved heat transfer with pin perforations leads to significantly reduced processor case temperatures and pin mass. Their experiments also revealed that practical considerations, including pin perforation alignment with the dominant flow direction and the quality of the pins' surface finish, can affect the heat transfer and pressure drop significantly.

Most studies of PHSs to date have considered cases where the pins have cross-sectional aspect ratios, AR≈1. The present study focusses on the benefits of employing pins with a larger aspect ratio, AR=2.25, as a compromise between the simplicity of PFHSs and the need

to employ several small pins on PHSs. Such heat sinks are referred to here as strip fin heat sinks (SFHSs) and very few previous studies of SFHSs have appeared in the literature. Jonsson and Moshfegh [23], for example, studied the performance of strip fins, square pins, circular pins, and plate fin with in-line and staggered arrangements. Using a coarse arrangement of strip fins with AR=5.3, the pressure drop in their experiments was substantially lower than for a denser arrangement of pins but with a similar thermal resistance. Hong and Cheng [24] studied the performance of strip fins in staggered arrangements in a micro-channel heat sink. They varied fin's length and the spaces between fins to find the optimal design. Their results showed that SFHSs clearly enhance the rate of heat transfer and that the pressure drop is strongly related to strip fin spacing.

The present study is the first detailed numerical investigation into the benefits of employing perforations in SFHSs. It compares the thermal and hydraulic performance of staggered and in-line arrangements of strip fins with PHSs with circular and square pins of AR=1, and shows how these can be further enhanced by perforating the strip fins. The paper is organised as follows. The paper is organised as follows. Section 2 describes the conjugate heat transfer model for the heat sink problems under consideration and the numerical methods used to solve them. A comprehensive set of solutions is presented in Section 3 and conclusions are drawn in Section 4.

2. NUMERICAL METHODS

2.1 Problem Description

The heat sink designs considered are shown in Fig 1 with circular and square pins, of cross-sectional aspect ratio AR=l/w=1, and strip fins with AR=2.25, where l, and w are length and width of fin respectively. Those values are chosen to facilitate a convenient comparison with the PHSs considered here. Heat sinks with solid and perforated fins in the in-line or staggered arrangements shown in Figure 2 are investigated. The perforated fins contain three circular perforations aligned with the direction of flow and the diameter of each perforation is 1 mm. The case with circular pins in an in-line arrangement has recently been studied by [15]. The dimensions of the base plate, fin height and fin thickness or diameter are the same for all heat sinks and are equal to 50×50 mm, 10 mm and 2 mm, respectively. The number of fins is 64 for those with in-line arrangement and 60 for heat sinks with staggered configuration. Following Al-Damook et al [15], the heat sinks are aluminium with thermal conductivity 202 W/m.K and with a base plate thickness of 2 mm.

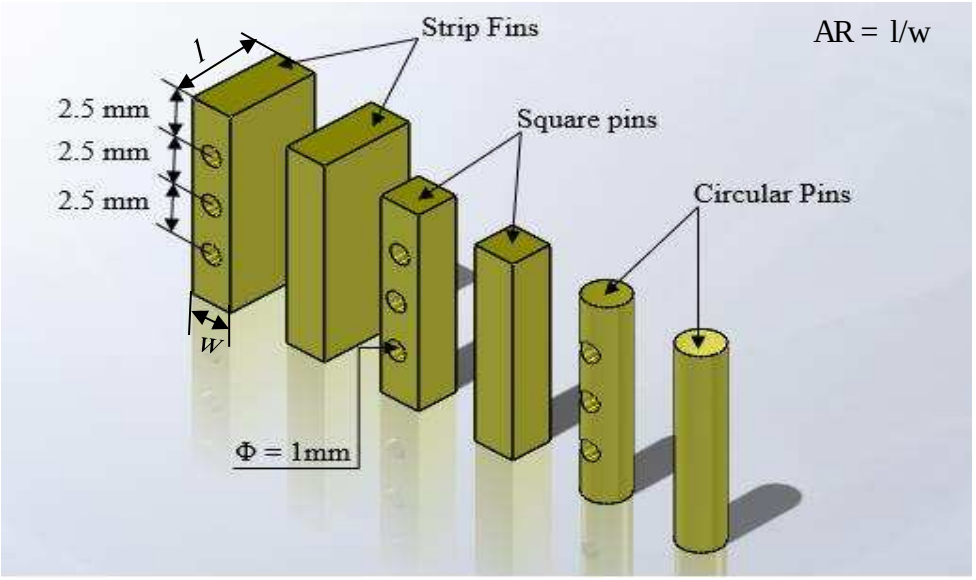

Figure 1: The six fin designs considered, and a definition of pin aspect ratio, AR=l/w.

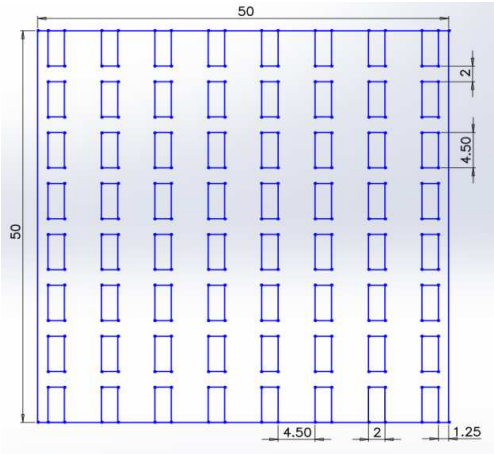

Strip fin with in-line arrangement

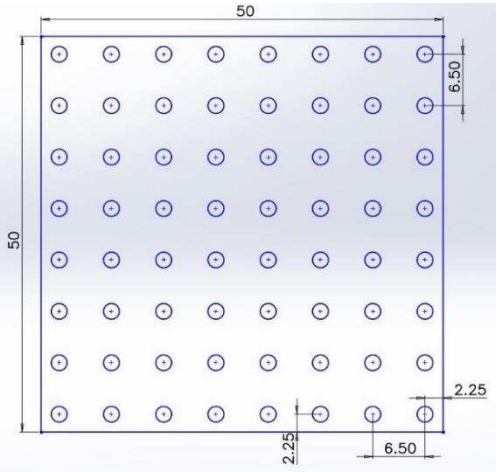

Circular pin fin with in-line arrangement

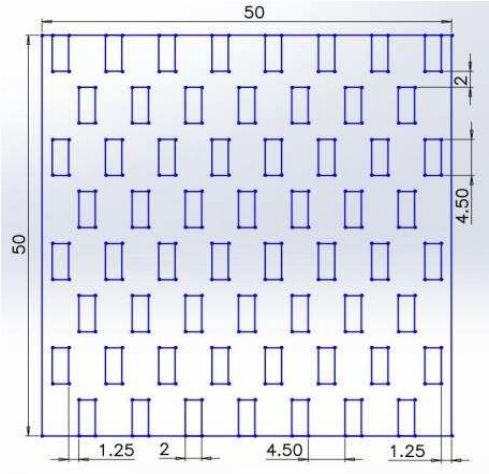

Strip fin with staggered arrangement

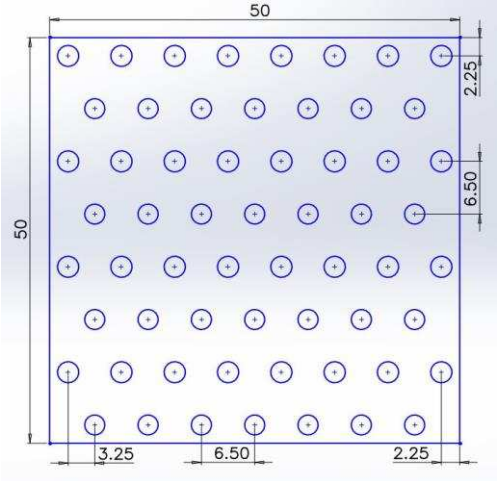

Circular pin fin with staggered arrangement

Figure 2: Schematic diagram of different heat sink geometries and arrangements.

2.2 Conjugate Heat Transfer Model

Following Al-Damook et al [15], a conjugate heat transfer model for the turbulent air flow over the heat sinks is developed with the properties of air based on the inlet temperature of 18^{o}C. The inlet velocity ranges between 6.5 m/s and 12 m/s which leads to Reynolds numbers between 3500 and 6580, based on equations (1) and (2).

$$R_e = \rho U D_h/\mu \tag{1}$$

$$D_h = 4\frac{A_c}{p} \tag{2}$$

The air flow is considered as steady state, incompressible and turbulent, see e.g. [11-13], and the conjugate heat transfer model analyses the heat flux which is transferred through the heat sink into the moving air through the coupled boundary condition shown in Fig. 3(a). The heat flux through the heat sink is computed by solving Fourier's conduction equation (3).

Zhou and Catton [25] modelled the turbulent air flow using the Reynolds-Averaged and Navier-Stokes (RANS) form of the continuity, momentum and energy equations (4, 5 and 7) respectively.

$$\nabla.(k_s \nabla T_s) = 0 \tag{3}$$

$$\nabla.\underline{U} = 0 \tag{4}$$

$$\frac{\partial \underline{U}}{\partial t} + \nabla.(\underline{U}\,\underline{U}) = \frac{1}{\rho}\nabla.\left(\underline{\underline{\sigma}} - \rho\overline{\underline{U}'}\,\overline{\underline{U}'}\right) \tag{5}$$

In equation (5) $\underline{\underline{\sigma}}$ is represented the Newtonian stress tensor which can be computed using equation (6).

$$\underline{\underline{\sigma}} = -p\underline{\underline{I}} + \mu\left(\nabla\underline{U} + [\nabla\underline{U}]^T\right) \text{ and } -\rho\overline{\underline{U}'}\,\overline{\underline{U}'} = \mu_t\left(\nabla\underline{U} + [\nabla\underline{U}]^T\right) - 2/3(\rho k\underline{\underline{I}}) \tag{6}$$

Where $\overline{\underline{U}'}$ and $\underline{U}$ are the fluctuation and average turbulent velocity vectors respectively, and p and $\underline{\underline{I}}$ represent the pressure and the unit tensor.

$$\frac{\partial T_f}{\partial t} + \underline{U}.\nabla T_f = \left(\frac{\nu}{Pr} + \frac{\nu_t}{Pr_t}\right)\nabla^2 T_f + \frac{Q}{\rho C_p} \tag{7}$$

Following a number of recent, successful models of thermal air flows over heat sinks, the k-ω SST model with automatic wall function treatment is used [15], [25]. The equations of this model are given in the following equations (9, 10, 11, 12, 13, 14 and 15):

$$\frac{\partial(\rho k)}{\partial t}+\underline{U}.\nabla(\rho k)=\tilde{P}_k-\beta^*\rho k\omega+\nabla.\left[(\mu+\sigma_k\mu_t)\nabla k\right] \tag{9}$$

$$\frac{\partial(\rho\omega)}{\partial t}+\underline{U}.\nabla(\rho\omega)=\alpha\rho S^2-\beta\rho\omega^2+\nabla.\left[(\mu+\sigma_\omega\mu_t)\nabla\omega\right]+2(1-F_1)\rho\sigma_{\omega_2}\frac{1}{\omega}\nabla k.\nabla\omega \tag{10}$$

In equation (10) $\boldsymbol{F_1}$ refers to blending function defined in equation (11), where $\boldsymbol{CD_{\omega k}}$ and the turbulent eddy viscosity $\boldsymbol{v_t}$ are specified in equations (12) and (13) respectively. $\boldsymbol{F_2}$ and $\boldsymbol{S}$ refer to the second blending function and invariant measure of the strain rate respectively and $\boldsymbol{F_2}$ is calculated using equation (14).

$$F_1=\tanh\left(\left\{\min\left[\max\left(\frac{\sqrt{k}}{\beta^*\omega y},\frac{500\nu}{y^2\omega}\right),\frac{4\rho\sigma_{\omega_2}k}{CD_{k\omega}y^2}\right]\right\}^4\right) \tag{11}$$

$$CD_{k\omega}=\max\left(2\rho\sigma_{\omega_2}\frac{1}{\omega}\nabla k.\nabla\omega,10^{-10}\right) \tag{12}$$

$$\nu_t=\frac{a_1 k}{\max(a_1\omega,SF_2)} \tag{13}$$

$$F_2=\tanh\left(\left[\max\left\{2\frac{\sqrt{k}}{\beta^*\omega y},\frac{500\nu}{y^2\omega}\right\}\right]^2\right) \tag{14}$$

Equation (15) is employed to limit the growth of flow stagnation regions.

$$P_k=\mu_t\frac{\partial u_i}{\partial x_j}\left(\frac{\partial u_i}{\partial x_j}+\frac{\partial u_j}{\partial x_i}\right)\rightarrow\tilde{P}_k=\min\left(P_k,10\beta^*\rho k\omega\right) \tag{15}$$

The constants for the SST model are taken as:

$$\beta^*=0.09,\alpha_1=\frac{5}{9},\beta_1=\frac{3}{40},\sigma_{k1}=0.85,\sigma_{\omega_1}=0.5,\alpha_2=0.44,\ \beta_2=0.0828,\sigma_{k2}=1,\sigma_{\omega 2}=0.856.$$

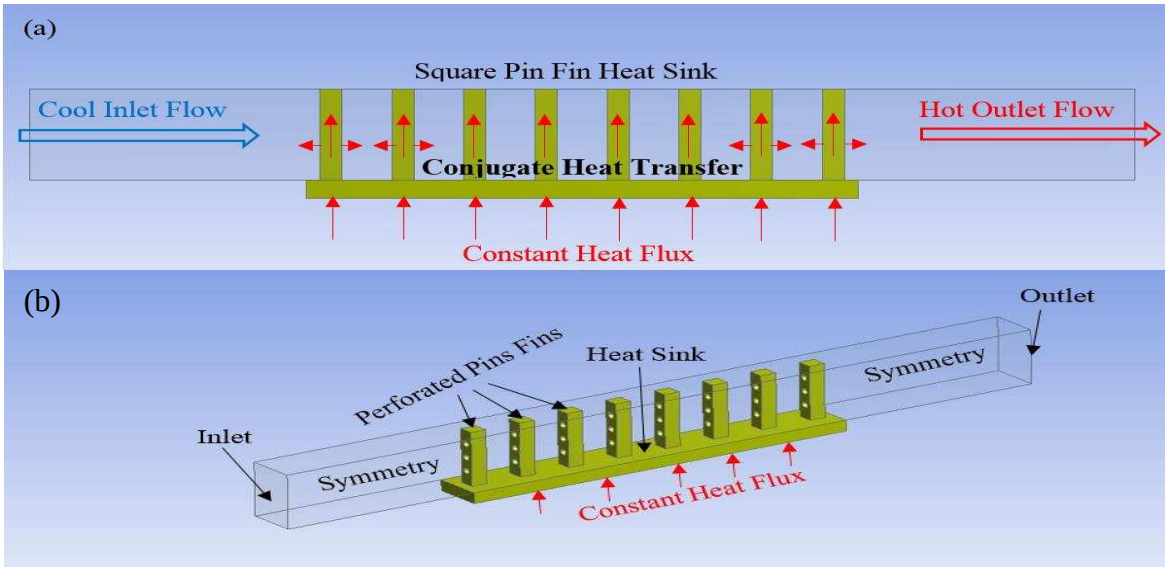

Figure 3: (a) Conjugate heat transfer process; (b) the flow domain.

2.3 Boundary Conditions

Following the experiments of Al-Damook et al [15], the following boundary conditions are used. Note that, due to symmetry, the flow through only one row of fins is analysed [11], see Fig. 3(b).

1- On the bottom of the heat sink a uniform heat flux of 20000 W/m^2 and a no-slip condition, U = 0 are applied.
2- The inlet fluid temperature is at 18^{o}C and its velocity ranges between 6.5 and 12 m/s.
3- The outlet pressure is equal to zero and the temperature gradient is zero ($\frac{dT}{dx} = 0$).
4- At the fin surfaces no slip, U = 0, and heat flux is conserved ($k_f . \frac{dTf}{dn} = k_s \frac{dT_s}{dn}$).
5- The left and right sides are taken to be symmetry boundaries.
6- All other walls, no slip and adiabatic conditions are applied.

Following a number of previous studies, e.g. [15], which have shown radiative heat transfer is small for the conditions considered here, radiative losses are neglected.

2.4 Grid Independent Test (GIT)

The effect of grid refinement on the numerical solutions is investigated for the cases of solid and perforated square pin fins in an in-line arrangement, see Table 1. The results for the perforated PHS show that increasing the number of cells above 755069 leads to a less than 0.5% variation in the base temperature and pressure drop. For solid fins, far fewer cells are needed and the results imply that grid independence is achieved with only 95410 cells.

Table 1 : Effect of grid density for a PHS with solid and perforated square pin fin in an in-line configuration

Geometry	Number of Cells	The base temperature (^{o}C)	Pressure drop (Pa)
Solid square PHS	45000	69.8	57
	64868	71.2	55.2
	95410	73.0	54.0
	118984	73.1	54.0
Perforated square PHS with three perforations	436422	58.0	44.0
	667851	65.3	38.5
	755069	67	36.0
	923254	67.2	36.0

3. Results and Discussion

3.1 Validation of the Numerical Method

The numerical solutions are next validated for the cases of solid circular pin fins in staggered arrangement and solid square pin fins in in-line arrangement studied experimentally by Yang et al. [18]. Fig. 4(a) compares the pressure drop (ΔP) and heat transfer coefficient (h) for the staggered, circular pins and the average discrepancies for pressure drop and heat transfer coefficient are 4% and 4.5% respectively. Fig. 4(b) presents the corresponding data the case with square pins in an in-line configuration; in this case the average discrepancies are 3% and 4.5% for pressure drop and heat transfer coefficient respectively.

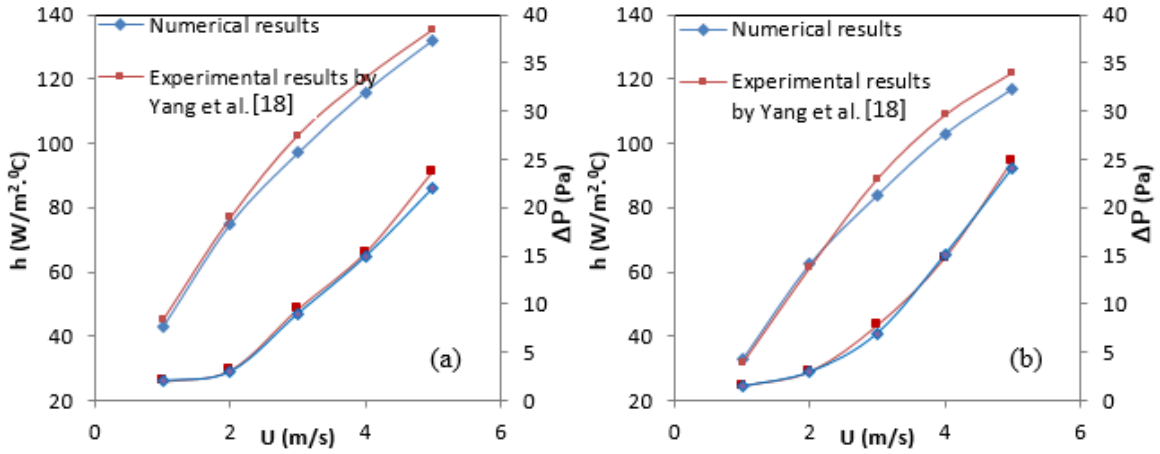

Figure 4: (a) validation for circular pin fin with staggered configuration; (b) validation for square pin fin with in-line arrangement.

3.2 Numerical comparisons of pressure drop in PHSs and SFHSs

Fig. 5 shows the pressure drop for solid and perforated fins in an in-line arrangement, which as expected demonstrates that it increases monotonically with air velocity. Fig. 5(a) presents the pressure drop for solid pins and it is clear that by far the largest pressure drops, typically 80% larger than the others, are for the square pins fins whereas those for the circular and strip fin are in very close agreement. The larger pressure drop for the square pins may be due to flow separation around the square pins which increases the associated pressure drag on them.

Fig. 5(b) shows the pressure drops for the perforated fins. These show clearly that the pressure drop decreases compared with the solid fins. The highest reduction is observed for square pins, which is typically around 12%, while the reductions for the circular pin and strip fins are typically around 6.5% and 9% respectively, with the strip fin having the smallest pressure drop.

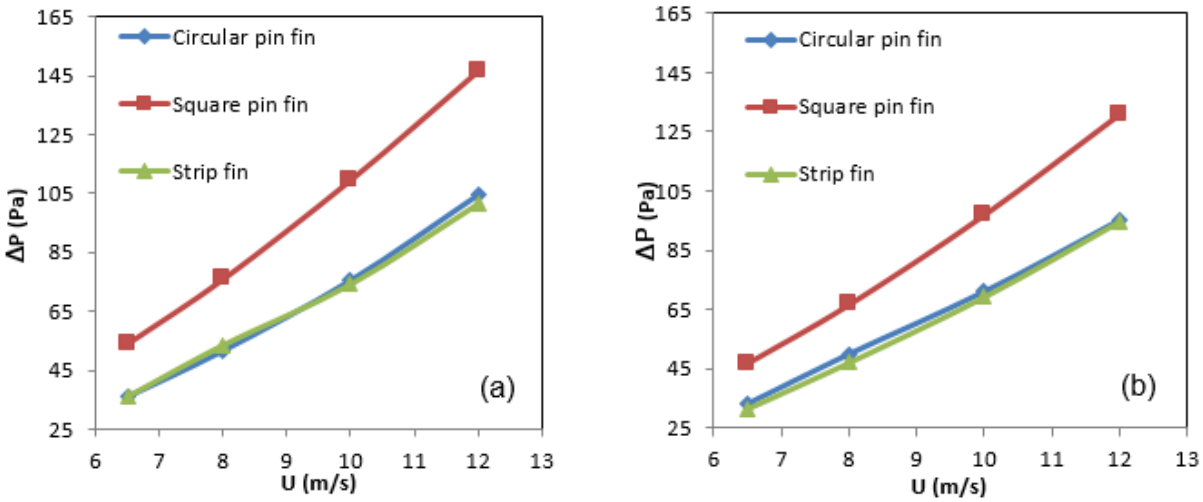

Figure 5: (a) pressure drop for solid fins with in-line arrangement; (b) pressure drop for perforated fins with in-line configuration

Fig. 6 shows that staggering the fins has a significant effect on pressure drop, increasing it substantially in all cases. The highest pressure drop in this case is for the strip fin, which increases by up to 80%, since the fins present a barrier to all regions of the airflow. Such blockage effects also result in average increases in pressure drop for the square and circular pins of approximately 63% and 33% respectively. Fig 6(b) shows that perforations lead to reductions in the pressure drop in all cases. For the circular, square and strip fins the average reduction in pressure drop are approximately 10%, 25% and 22% respectively. It is clear that perforations are more beneficial when fins are staggered.

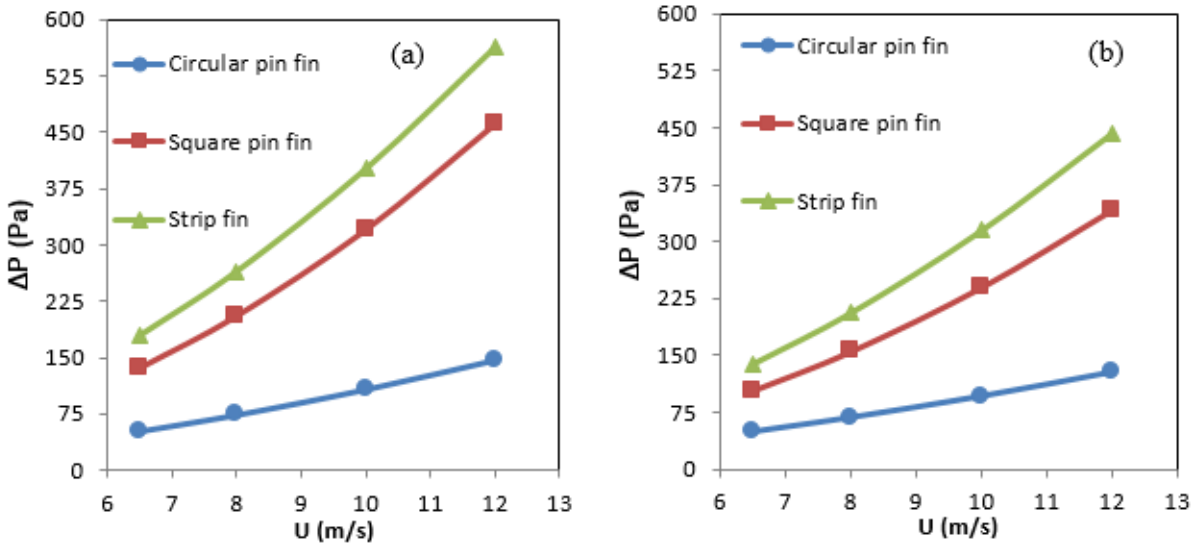

Figure 6: (a) pressure drop for solid fins with staggered arrangement; (b) pressure drop for perforated fins with staggered arrangement

3.3 Numerical comparisons of heat transfer coefficient

The heat transfer coefficient of a heat sink depends on the choice of characteristic area used. Al-Damook et al [15] have recently shown that using the heat transfer coefficient, h_p based on the projected cross-sectional area of the heat sink that calculated using $h_p = \frac{\dot{Q}}{A_p\left[T_W - \left(\frac{T_{out}+T_{in}}{2}\right)\right]}$ is perhaps the most useful indicator of the heat transfer efficiency for practical considerations, where $A_p = WL$ the projected base area, L and W are length and width of heat sink respectively. Fig. 7(a) shows predictions of h_p with the fins in an in-line configuration and demonstrates that the strip fins provide the largest rates of heat transfer. It is likely that this is mainly due to its larger wetted area in contact with the air, compared with pin fins. The effect of perforations is shown in Fig. 7(b); they are seen to enhance heat transfer significantly, with increases of the order of 20-25% for all cases considered. This is probably due to not only its larger wetted area in contact with the air, compared with pin fins, but also due to the effect of localised air jets that pass through the fins and reduce the size of recirculating regions behind them, see e.g. [15].

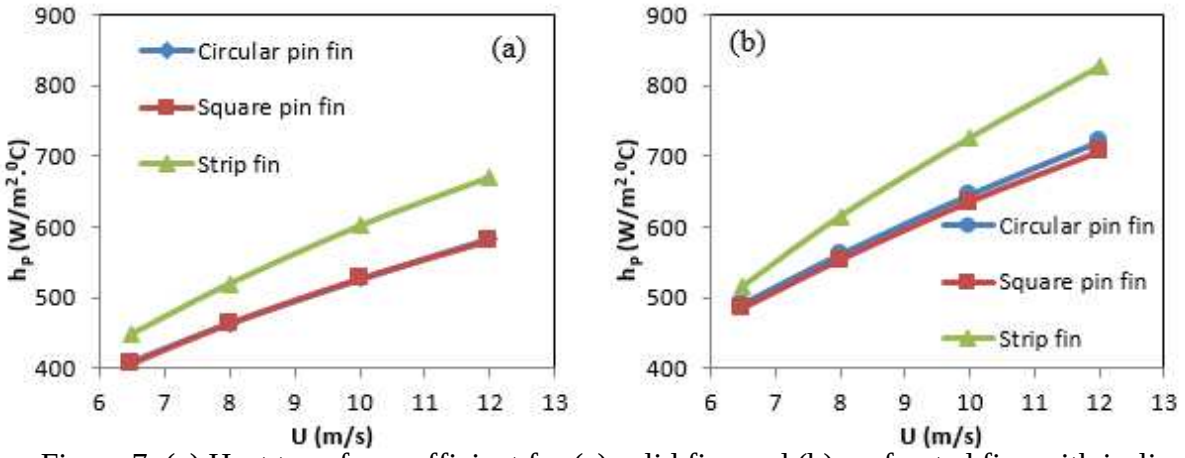

Figure 7: (a) Heat transfer coefficient for (a) solid fins and (b) perforated fins with in-line arrangement.

Figure 8 demonstrates that staggering the fins increases the heat transfer coefficients significantly, with typically increases of around 50%, 20% and 10% for the strip, square pin and circular pin fins respectively. Staggering the strips breaks down the boundary layer very effectively, generating higher levels of turbulent heat transfer. Perforating the fins increases the rates of heat transfer yet further, with enhancements typically between 20 and 30% being realised.

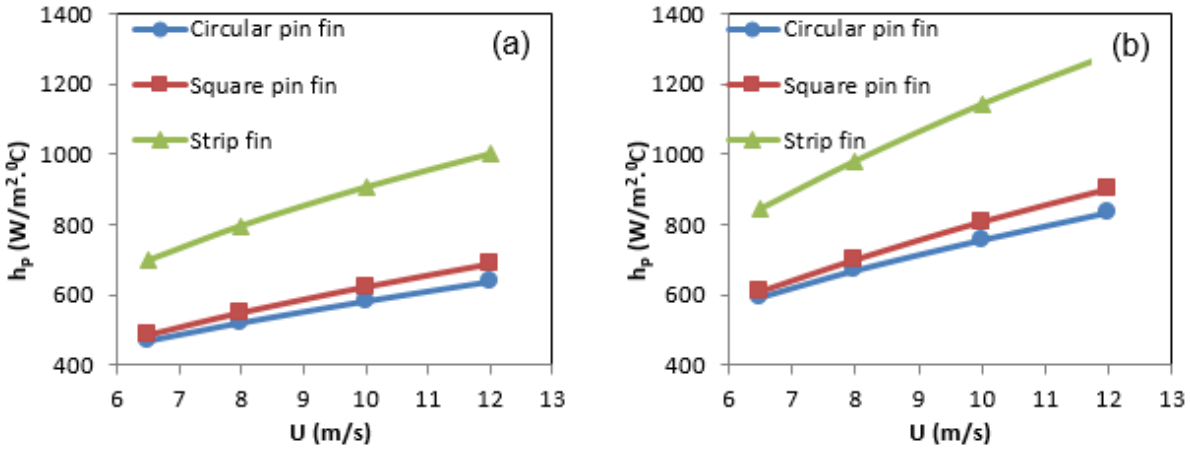

Figure 8: Heat transfer coefficient for (a) solid fins and (b) perforated fins with staggered arrangement.

3.4 Numerical predictions of heat sink base temperature

The primary goal of the heat sink in electronic systems is to ensure that the processor temperatures remain below critical temperatures to avoid component damage and failure. For PCs, for example, Yuan et al. [26] stated that this critical temperature is around 85^{o}C. The effects of inlet air flow velocity and fin perforations on T_{base} are shown in Fig. 9. For an in-line fin arrangement with solid pins, Fig. 9(a) shows that the T_{base} values are very similar for the square and circular pins, whereas the improved heat transfer from the strip fins reduces T_{base} by typically 5-6^{o}C. Fig. 9(b) shows that the improved heat transfer from perforating the fins reduces all T_{base} values by typically 3-4^{o}C. The substantial improvements in heat transfer from staggering the fins are also demonstrated in Figs. 9(c) and 9(d). The former shows that staggering the solid strip fins reduces T_{base} by between 15 and 20^{o}C, for the solid square pins by 8-10^{o}C and for the solid circular pins by 5-8^{o}C, the latter having the poorest rates of heat transfer. The further reductions in T_{base} by perforating the fins lead are typically around 3-4^{o}C for the strip fins, typically 4-5^{o}C for the circular pins, and has very little effect for the square pin fins.

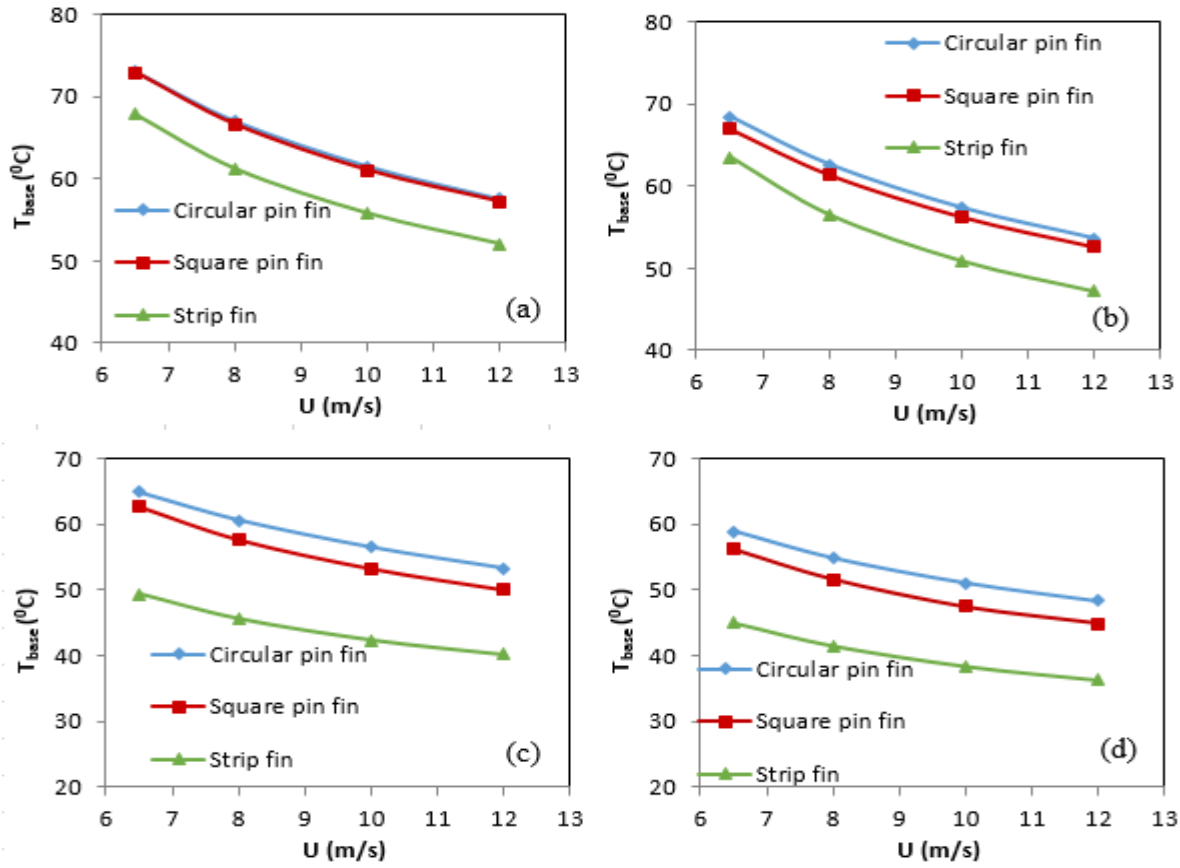

Figure 9: (a) T_{base} for solid models with in-line arrangement; (b) T_{base} for perforated models with in-line arrangement; (c) T_{base} for solid heat sinks with staggered arrangement; (d) T_{base} for perforated heat sinks with staggered arrangement.

3.5 Influence of perforations on the flow and temperature fields

Figure 10 shows how perforations alter the flow field around the strip fins for an in-line arrangement. These show that perforating the strip fins reduces the size of the recirculation region behind the fins, which acts to reduce the overall pressure drop. The enhancement in the rate of heat transfer is due to the combination of the increase in the wetted area in contact with the air and the creation of localised jets that lead to higher convective heat transfer, see also Al-Damook et al [15].

Examples of temperature fields on the SFHSs for solid and perforated SFHSs with in-line and staggered arrangements of fins are presented in Fig. 11. The lowest T_{base}, corresponding to the lightest shade of green, is obtained for the perforated SFHSs in a staggered configuration. The figure demonstrates clearly that the perforated cases have the lowest surface temperature for a given fin arrangement.

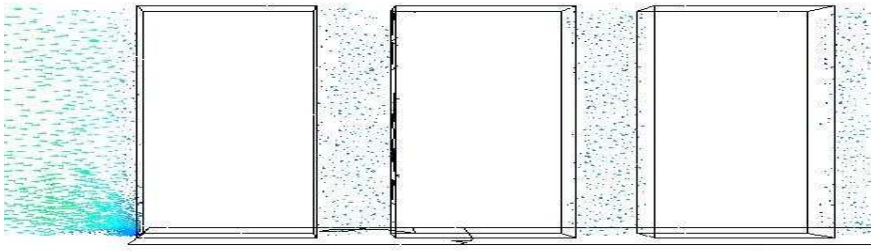

Solid strip fins

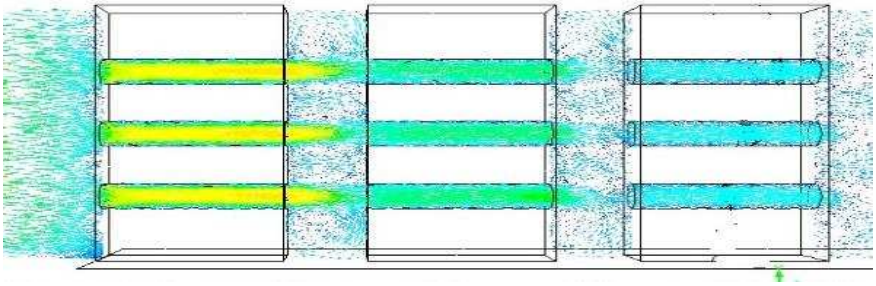

Perforated strip fins

Figure 10: Effect of perforation on fluid flow in the SFHSs.

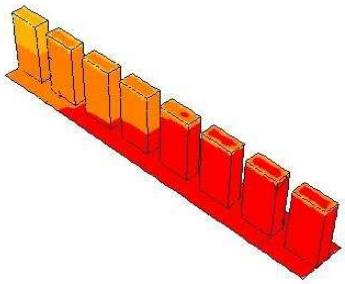

Solid SFHSs with in-line configuration

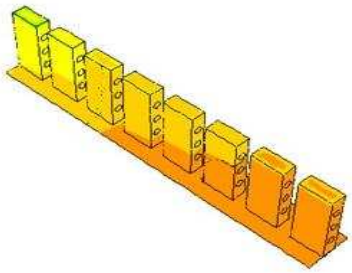

Perforated SFHSs with in-line configuration

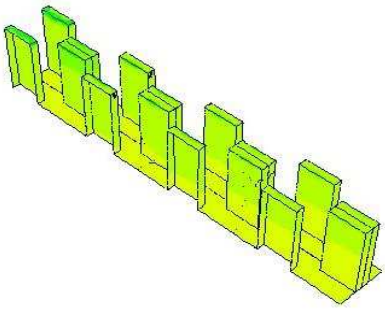

Solid SFHSs with staggered configuration

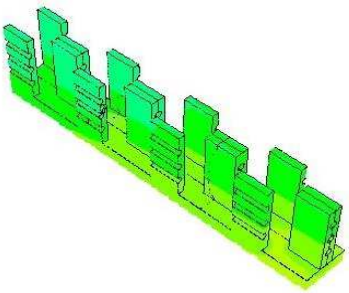

Perforated SFHSs with staggered configuration

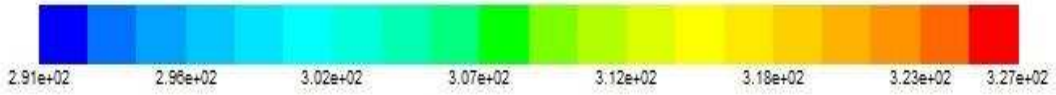

Figure 11: Temperature gradient for solid and staggered SFHSs with different configuration

3.6 Heat sink mass

Heat sinks are designed to be light as possible, while meeting their functional requirements on heat transfer and pressure drop, in order to reduce material consumption and increase portability. The total mass of the heat sinks considered here has been calculated utilising equations 16 and 17 and the values are showed in Table 2, where the density of aluminium $\rho_{Al} = 2712$ Kg/m3.

$$V_t = V_{base} + V_{fins} \tag{16}$$

$$m_t = \rho_{Al} \times V_t \tag{17}$$

Table 2: Masses of the examined heat sinks.

Model	Mass of solid geometry (g)	Mass of perforated geometry (g)	Reduction percentage
Circular pin fin	19.0	18.24	4.0%
Square pin fin	20.5	19.75	3.8%
Strip fin	29.2	27.40	6.2%

Table 2 shows that using perforated fins on heat sinks offer the additional advantage of a significant reduction in its mass, which for SFHSs is over 6%.

3 Conclusion

Heat sinks with surface fins provide critical cooling in a range of important industries and practical applications and are ubiquitous throughout the electronics industry. A large number of previous studies have analysed the benefits of plate fins and pins, with aspect ratios, while far fewer have considered employing strip fins with cross-sectional aspect ratios typically > 2 Strip fins can be extremely effective in breaking up the boundary layer and the combination of increased fin wetted surface area and increased turbulence can provide substantial enhancements in heat transfer, albeit with increased pressure losses. Staggering the strip fins enhances the heat transfer, with larger pressure losses. The present study is the first to show that perforating the strip fins provides an effective and practical means of enhancing heat transfer yet further with additional, significant benefits in terms of reduced pressure losses and heat sink mass and materials consumption.

There is great scope for achieving better heat transfer and pressure drop characteristics through formal optimisation of the perforated strip fin heat sinks and the arrangement of the fins. This work is currently ongoing.

4 References

[1]S. Gurrum, S. Suman, Y. Joshi and A. Fedorov, "Thermal Issues in Next-Generation Integrated Circuits", IEEE Transactions on Device and Materials Reliability, vol. 4, no. 4, pp. 709-714, 2004.

[2]M. Hajmohammadi, V. Alizadeh Abianeh, M. Moezzinajafabadi and M. Daneshi, "Fork-shaped highly conductive pathways for maximum cooling in a heat generating piece", Applied Thermal Engineering, vol. 61, no. 2, pp. 228-235, 2013.

[3]P. Hopton and J. Summers, "Browse Conference Publications > Semiconductor Thermal Measure ... Help Working with Abstracts Enclosed liquid natural convection as a means of transferring heat from microelectronics to cold plates", Semiconductor Thermal Measurement and Management Symposium (SEMI-THERM), 2013 29th Annual IEEE, pp. 60 - 64, 2013.

[4]A. McWilliams, "The Market for Thermal Management Technologies - SMC024G", Bccresearch.com, 2015. [Online]. Available: http://www.bccresearch.com/market-research/semiconductor-manufacturing/thermal-management-technologies-market-smc024g.html. [Accessed: 22- Dec- 2015].

[5]N. Nagarani, K. Mayilsamy, A. Murugesan and G. Kumar, "Review of utilization of extended surfaces in heat transfer problems", Renewable and Sustainable Energy Reviews, vol. 29, pp. 604-613, 2014.

[6]K. Chiang, "Optimization of the design parameters of Parallel-Plain Fin heat sink module cooling phenomenon based on the Taguchi method", International Communications in Heat and Mass Transfer, vol. 32, no. 9, pp. 1193-1201, 2005.

[7]H. Najafi, B. Najafi and P. Hoseinpoori, "Energy and cost optimization of a plate and fin heat exchanger using genetic algorithm", Applied Thermal Engineering, vol. 31, no. 10, pp. 1839-1847, 2011.

[8]M. Behnia, D. Copeland and D. Soodphakdee, "A comparison of heat sink geometries for laminar forced convection: numerical simulation of periodically developed flow", Thermal and Thermomechanical Phenomena in Electronic Systems, pp. 310-315, 1998.

[9]A. Dhumne and H. Farkade, 'Heat transfer analysis of cylindrical perforated fins in staggered arrangement', International Journal of Engineering Science and Technology (IJEST), vol. 6, pp. 125-138, 2013.

[10]I. Kotcioglu, A. Cansiz and M. Nasiri Khalaji, "Experimental investigation for optimization of design parameters in a rectangular duct with plate-fins heat exchanger by Taguchi method", Applied Thermal Engineering, vol. 50, no. 1, pp. 604-613, 2013.

[11]M. Shaeri and M. Yaghoubi, "Numerical analysis of turbulent convection heat transfer from an array of perforated fins", International Journal of Heat and Fluid Flow, vol. 30, no. 2, pp. 218-228, 2009.

[12]K. H. Dhanawade and H. S. Dhanawade, "Enhancement of Forced Convection Heat Transfer from Fin Arrays with Circular Perforation". IEEE, Frontiers in Automobile and Mechanical Engineering (FAME), pp. 192-196, 2010.

[13]M. Ismail, "Effects of Perforations on the Thermal and Fluid Dynamic Performance of a Heat Exchanger", IEEE Transactions on Components, Packaging and Manufacturing Technology, vol. 3, no. 7, pp. 1178-1185, 2013.

[14]D. Soodphakdee, M. Behnia, D.W. Copeland, "A comparison of fin geometries for heat sinks in laminar forced convection Part I: round elliptical, and plate fins in staggered and in-line configurations", Int. J. Microcircuits Electron. Packag, vol. 24, pp. 68-76, 2001.

[15]A. Al-Damook, N. Kapur, J. Summers and H. Thompson, 'An experimental and computational investigation of thermal air flows through perforated pin heat sinks', Applied Thermal Engineering, vol. 89, pp. 365-376, 2015.

[16]H. Shaukatullah, W. Storr, B. Hansen and M. Gaynes, "Design and optimization of pin fin heat sinks for low velocity applications", IEEE Transactions on Components, Packaging, and Manufacturing Technology: Part A, vol. 19, no. 4, pp. 486-494, 1996.

[17]N. Sahiti, A. Lemouedda, D. Stojkovic, F. Durst and E. Franz, "Performance comparison of pin fin in-duct flow arrays with various pin cross-sections", Applied Thermal Engineering, vol. 26, no. 11-12, pp. 1176-1192, 2006.

[18]Y. Yang and H. Peng, "Numerical study of pin-fin heat sink with un-uniform fin height design", International Journal of Heat and Mass Transfer, vol. 51, no. 19-20, pp. 4788-4796, 2008.

[19]P. Naphon and A. Sookkasem, "Investigation on heat transfer characteristics of tapered cylinder pin fin heat sinks", Energy Conversion and Management, vol. 48, no. 10, pp. 2671-2679, 2007.

[20]B. Sahin and A. Demir, “Thermal performance analysis and optimum design parameters of heat exchanger having perforated pin fins”, Energy Conversion and Management, vol. 49, no. 6, pp. 1684-1695, 2008.
[21]B. Sahin and A. Demir, “Performance analysis of a heat exchanger having perforated square fins”, Applied Thermal Engineering, vol. 28, no. 5-6, pp. 621-632, 2008.
[22]X. Dai, F. Yang, R. Fang, T. Yemame, J. Khan and C. Li, "Enhanced single- and two-phase transport phenomena using flow separation in a microgap with copper woven mesh coatings", Applied Thermal Engineering, vol. 54, no. 1, pp. 281-288, 2013.
[23]H. Jonsson and B. Moshfegh, “Modeling of the thermal and hydraulic performance of plate fin, strip fin, and pin fin heat sinks-influence of flow bypass”, IEEE Transactions on Components and Packaging Technologies, vol. 24, no. 2, pp. 142-149, 2001.
[24]F. Hong and P. Cheng, "Three dimensional numerical analyses and optimization of offset strip-fin microchannel heat sinks", International Communications in Heat and Mass Transfer, vol. 36, no. 7, pp. 651-656, 2009.
[25]F. Zhou and I. Catton, “Numerical Evaluation of Flow and Heat Transfer in Plate-Pin Fin Heat Sinks with Various Pin Cross-Sections”, Numerical Heat Transfer, Part A: Applications, vol. 60, no. 2, pp. 107-128, 2011.
[26]W. Yuan, J. Zhao, C. Tso, T. Wu, W. Liu and T. Ming, 'Numerical simulation of the thermal hydraulic performance of a plate pin fin heat sink', Applied Thermal Engineering, vol. 48, pp. 81-88, 2012.